1951 BIENNIAL INSPECTION

FATIGUE OF AIRCRAFT STRUCTURES

Presented by

Norris F. Dow
Herbert F. Hardrath
Charles B. Landers
Arthur J. McEvily, Jr.

Most of you have ridden in airplanes and experienced the disagreeable forces associated with flight through rough air. Those same forces which you felt as a passenger were also felt by the airplane as stresses in its structure.

It is well known that repeated stressing of material may eventually cause the material to fail even though the stresses are far below the ultimate strength of the material. This type of failure is known as fatigue failure. Although the reasons why materials fail by fatigue are not yet fully understood, many factors affecting the fatigue life of structures are known. For example, fatigue cracks generally start in the vicinity of so-called stress raisers such as notches, holes, or fillets, which interrupt the uniform flow of stresses through the structure. The action of such a stress raiser will be demonstrated with a specimen like this one, but 12-feet-long, in the one million-pound-capacity testing machine. The specimen contains a notch at the middle of each side edge. Electrical wire strain gages have been attached to the specimen across the section between the notches. These gages are connected to this strain indicating apparatus. The operator will apply tension loads to the ends of the specimen. The strains are indicated by these standpipes. The strains immediately adjacent to the notch, where the stress is highest, are indicated by the end standpipes, the strain in the center of the panel by the center standpipes, thus producing a bar graph representing the strain distribution across the specimen. Note that the strains at the edges are approximately four times those near the center where the stress is uniform. Accordingly, we would say that the stress concentration factor for this specimen is four. The operator will now release the load from the specimen.

The relation between the stress concentration factor and fatigue strength is affected by the absolute size of the specimen. Fatigue tests are usually run on small specimens like this rather than the size of the one in the testing machine. Consequently, in order to utilize the tests on the small specimens for designing full-scale structures, the size effect must be taken into account. We have found from tests of steel specimens that this empirical formula can be used to correlate fatigue results for specimens of different sizes. The fatigue stress concentration factor, K_n , is given in terms of the elastic stress concentration factor, K_t , determined for large specimens, and a ratio A/R ; where A is a critical dimension associated with the material itself and defined by this curve, and R is the radius at the base of the notch. While these results for the study of size effect have been obtained only for steel, work is under way on a similar study for aluminum alloys.

In the conventional type of fatigue test the repeated stresses are of constant amplitude and frequency as indicated by these plots of stress against time.

In flight, however, the stresses in the airplane structure depend on the gusts that are encountered and are consequently variable in amplitude and frequency. This curve is characteristic of stress records taken during flights in rough air.

In order to design airplanes to withstand the variable amplitude type of loading we must evaluate the cumulative effects of such loading.

One basic study on the effects of cumulative damage is being conducted with rotating beam type machines. These machines apply a given stress 10,000 times a minute and are equipped with motor driven cams which vary the applied load slowly. The stress pattern is therefore of the type schematically shown on this sketch.

Another fatigue testing machine which we are developing is capable of more closely simulating the variable stresses that actually occur in airplanes, such as those shown here. This machine applies a steady load corresponding to the load on an airplane wing during steady flight through smooth air. Then oscillating loads of 16 different amplitudes are superposed on the steady load. The amplitudes and the number of oscillations at each amplitude are selected before each test. Very complicated load patterns can thus be applied, and, in use, we adjust the pattern to agree with the statistical distribution of rough air loads.

This machine will now be demonstrated for you. Vertical loads will be applied to the specimen by this beam which is actuated by a hydraulic mechanism inside this box. The loads are controlled by the electronic apparatus in the tall black cabinet. Any desired sequence of application of dynamic loads may be obtained by appropriately punching the teletype tape which schedules the test. I will now start the machine.

The specimen in the machine is representative of one of the spars in a wing. The load is applied at the center and at both ends of the beam. The magnitude of the load at any time is indicated by the flashing lights in this column. The green light represents the mean load.

The wrinkles in this beam are somewhat more severe than those that occur in aircraft. The stresses, however, are not as severe as you might expect. This specimen has been loaded like this many times and I trust it will last for a number of additional demonstrations.

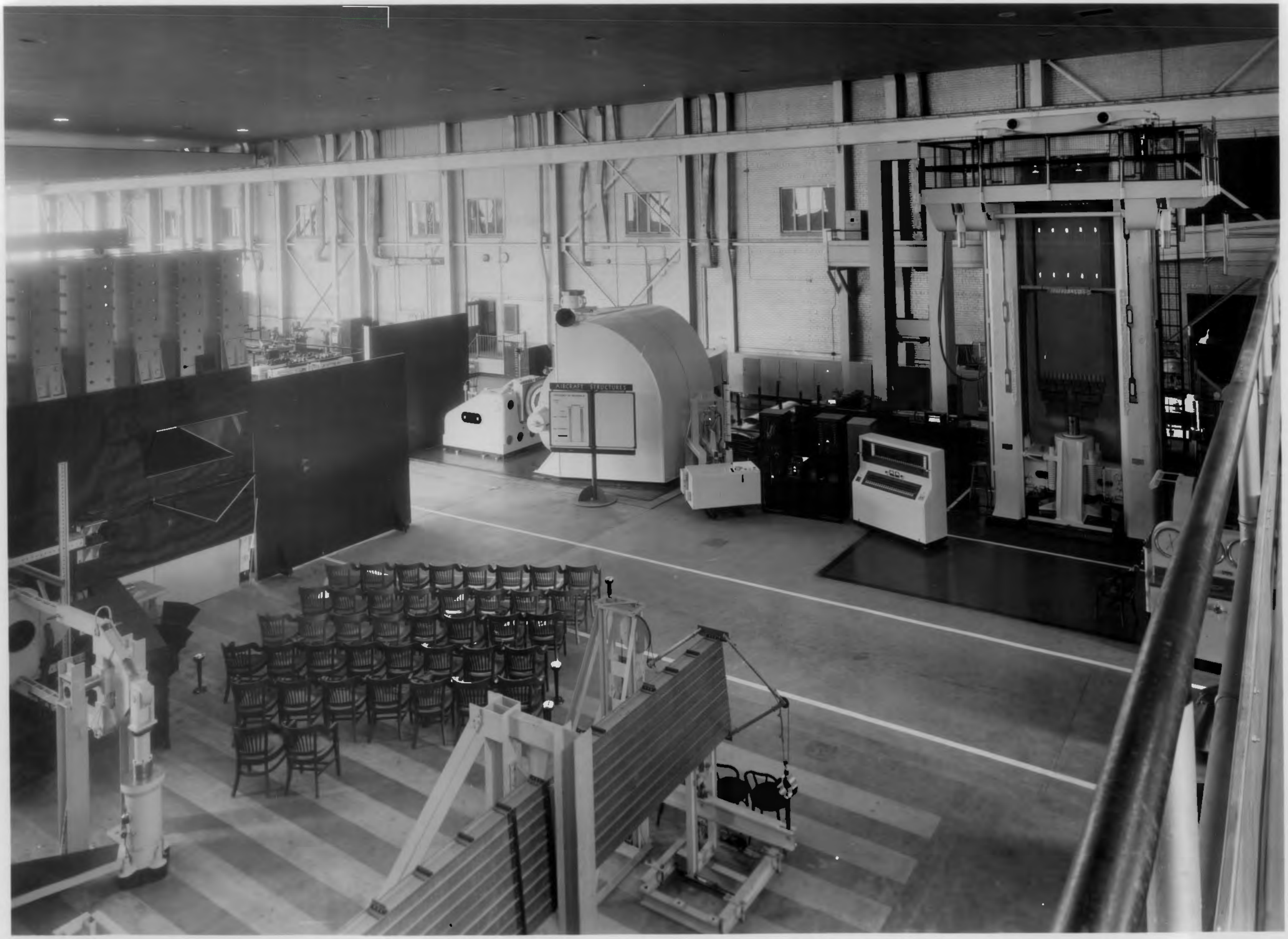

NACA

LAL 70594

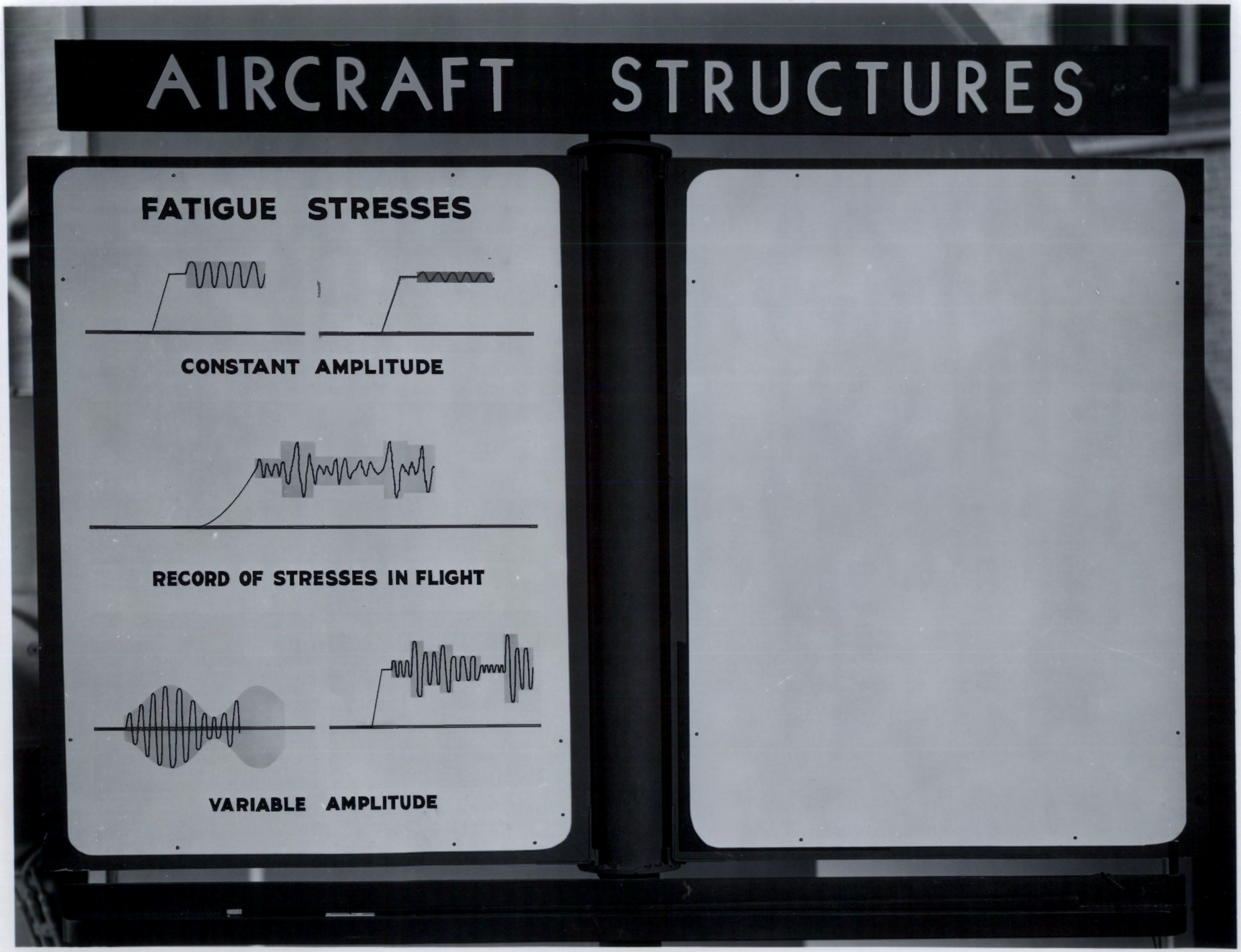

NACA

LAL 70604

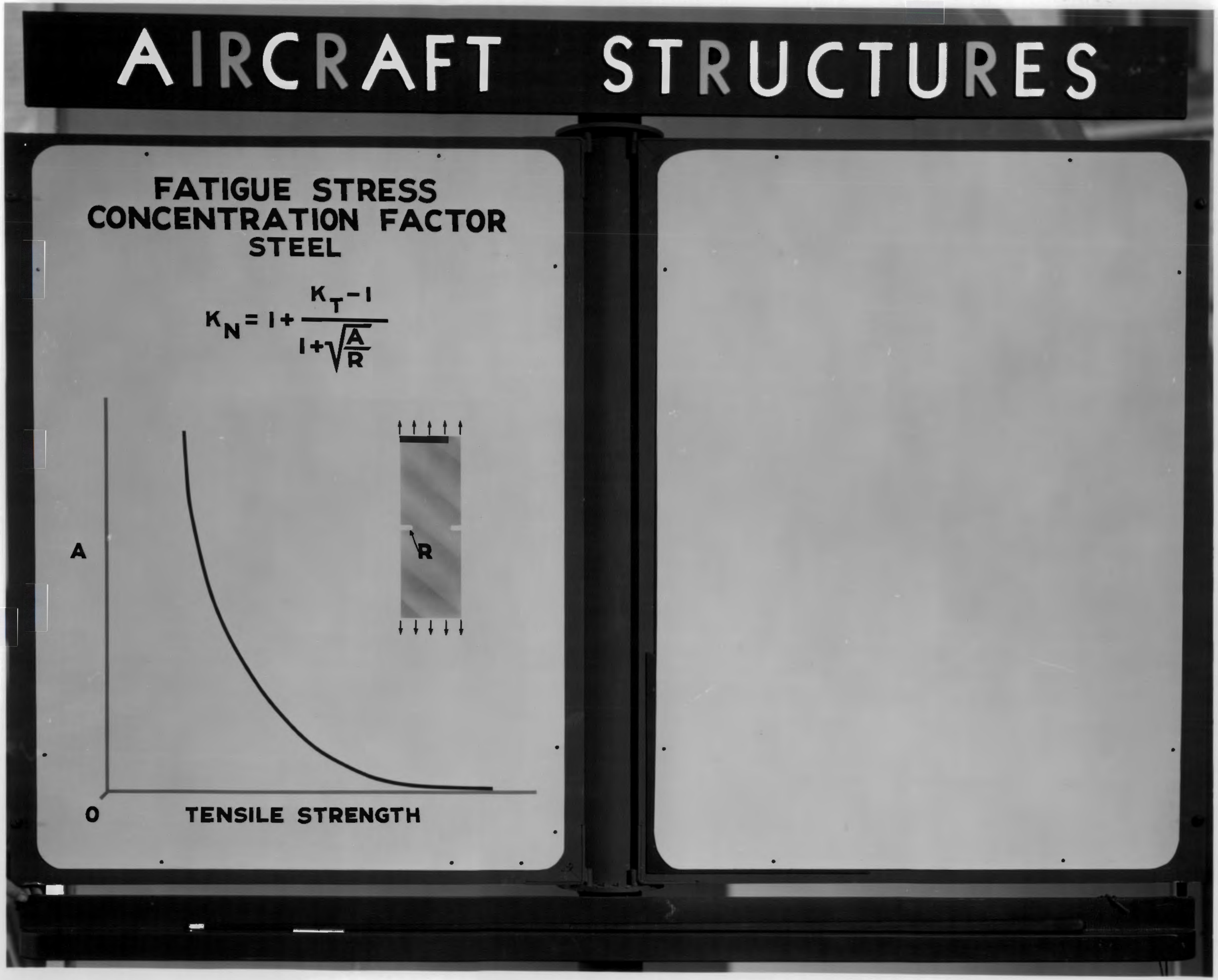

NACA
LAL 70602

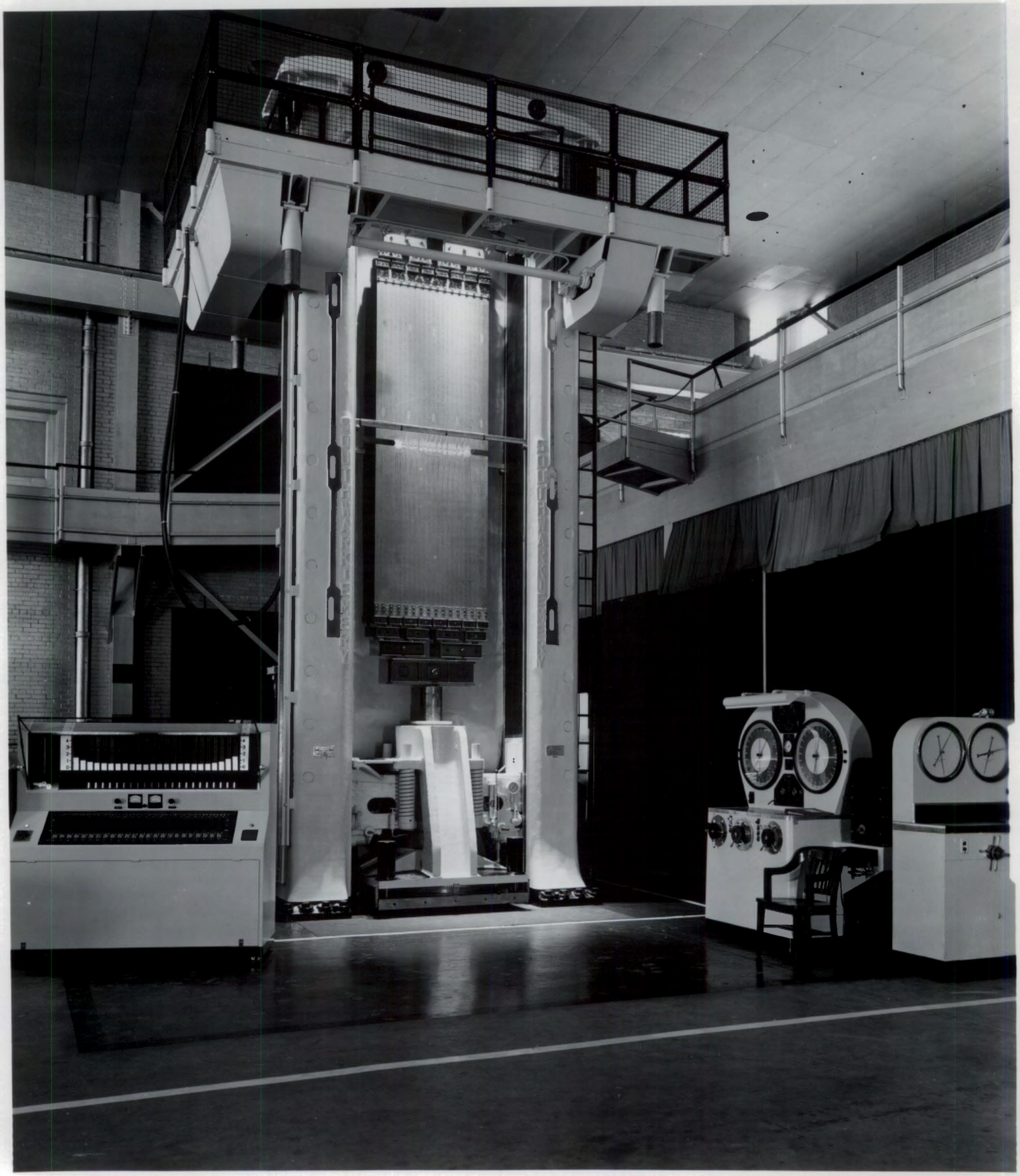

NACA

LAL 70591

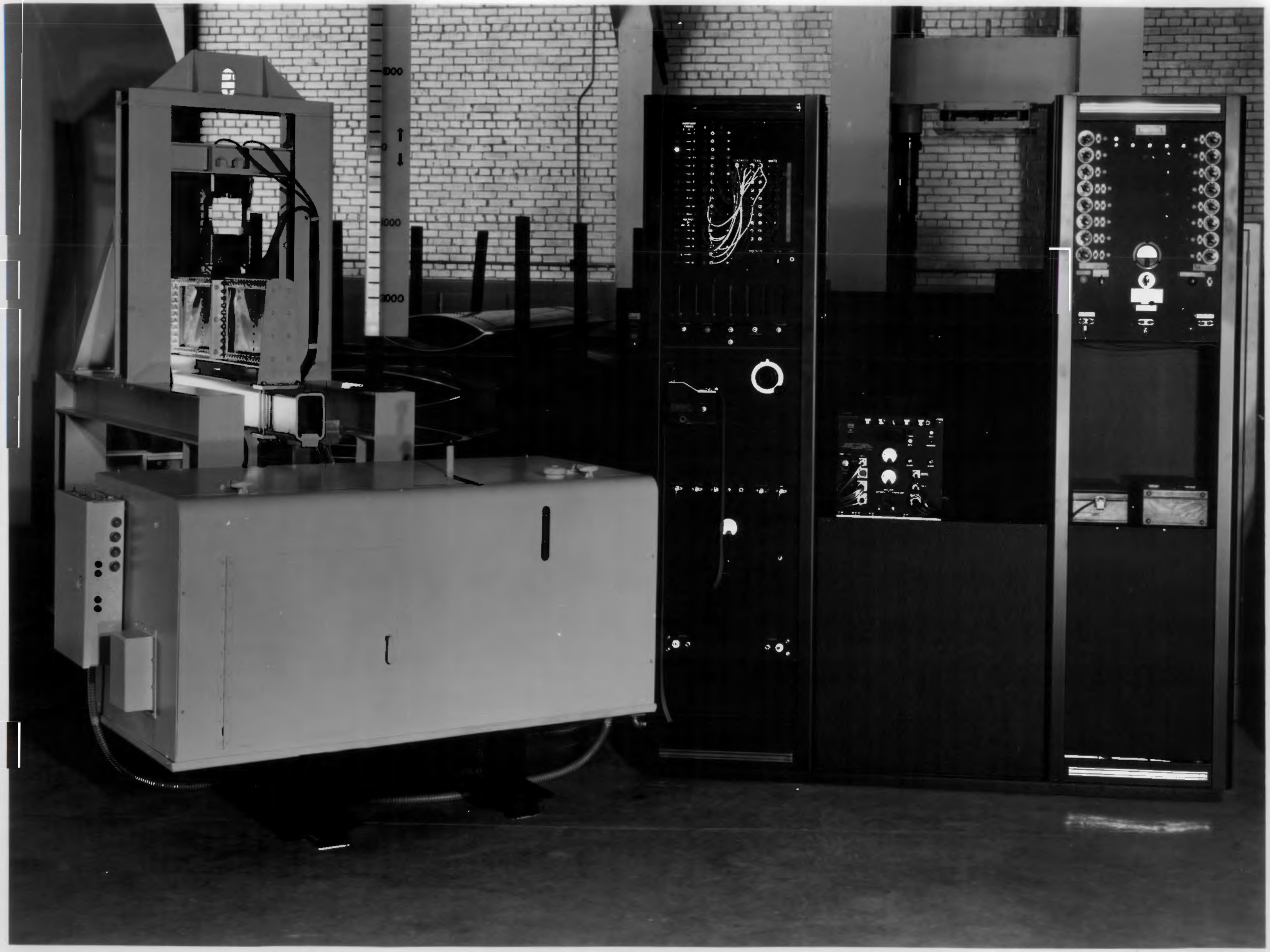

NACA
LAL 70592

1951 BIENNIAL INSPECTION

SELECTION OF MOST EFFICIENT STRUCTURAL MATERIALS FOR USE AT ELEVATED TEMPERATURES

Presented by

Charles Libove
Richard A. Pride
George E. Griffith
William M. Roberts
Aldie E. Johnson, Jr.

The effect of temperature on the material strength of several structural alloys is indicated in the upper part of this chart. The yield strength - i.e., the load the material is capable of carrying without exceeding a certain permanent deformation - is plotted against temperature. The aluminum alloys currently used in aircraft have lost a good part of their strength at 600° F. The titanium alloy and the stainless steel hold up much better. Stainless steel seems to have a marked superiority to titanium alloy according to this chart. The superiority is not so great, however, when we consider that steel is about 70 percent heavier than titanium. Saving weight is so very important for aircraft that we should really compare materials on the basis of strength per unit of weight. When this is done by dividing yield strength by the density of the material we see that stainless steel and titanium alloy are more nearly equivalent, with titanium being better at the lower temperatures and stainless steel somewhat better at the higher temperatures. 75S aluminum alloy now is comparable with the titanium alloy up to about 300° F.

A chart such as this gives the answer to the problem of material selection provided the material is put to a structural use in which it can develop its full yield strength - e.g., in a tension member such as the lower surface of a wing. In a compression structure like the plate elements in the upper skin of a wing the full material strength often cannot be realized because the skin tends to wrinkle. When the skin is thin this wrinkling can occur long before the material itself has been stressed to its capacity. After wrinkling occurs the plate elements can still take load but their maximum strength is no longer related in a simple way to the strength of the material.

For this reason another phase of our research has been devoted to establishing a correlation between the strength of a structural element that wrinkles and the yield strength of the material from which it is made. Such a correlation for plate compression elements is shown in the next chart. Here a single curve gives the strength of a plate element in terms of the yield strength of the material. This curve was established by extensive tests on many materials. Tests on one material were carried up to 600°. To enter the chart, we first have to compute the wrinkling stress of the plates which is easily done by methods well established in recent years.

If now we add considerations of weight to the information given by this chart, we can pick out the best material to use for the plate compression elements. The results are shown on the next chart. At temperatures above 800° stainless steel is the best of the several materials compared, the titanium alloy becoming superior in the intermediate temperature range. At the lower temperatures any one of three materials, titanium, aluminum, or magnesium, may be most efficient, depending upon the particular design conditions. For comparison we have shown on the right-hand side of the charts the previously discussed results for members in which the full yield strength of the material could be utilized such as tension members. As we recall, stainless steel is superior over most of the elevated temperature range. At temperatures up to about 300° aluminum alloy and the titanium alloy are about equally efficient. This chart illustrates that no one material is universally superior to all others for use at elevated temperatures. Rather, the choice of a material depends on its structural use.

Material-selection studies of the kind described are being extended to cover other high-temperature resistant materials and various structural elements; the objective being to enable the designer to select the most efficient materials quickly in the early design stages.

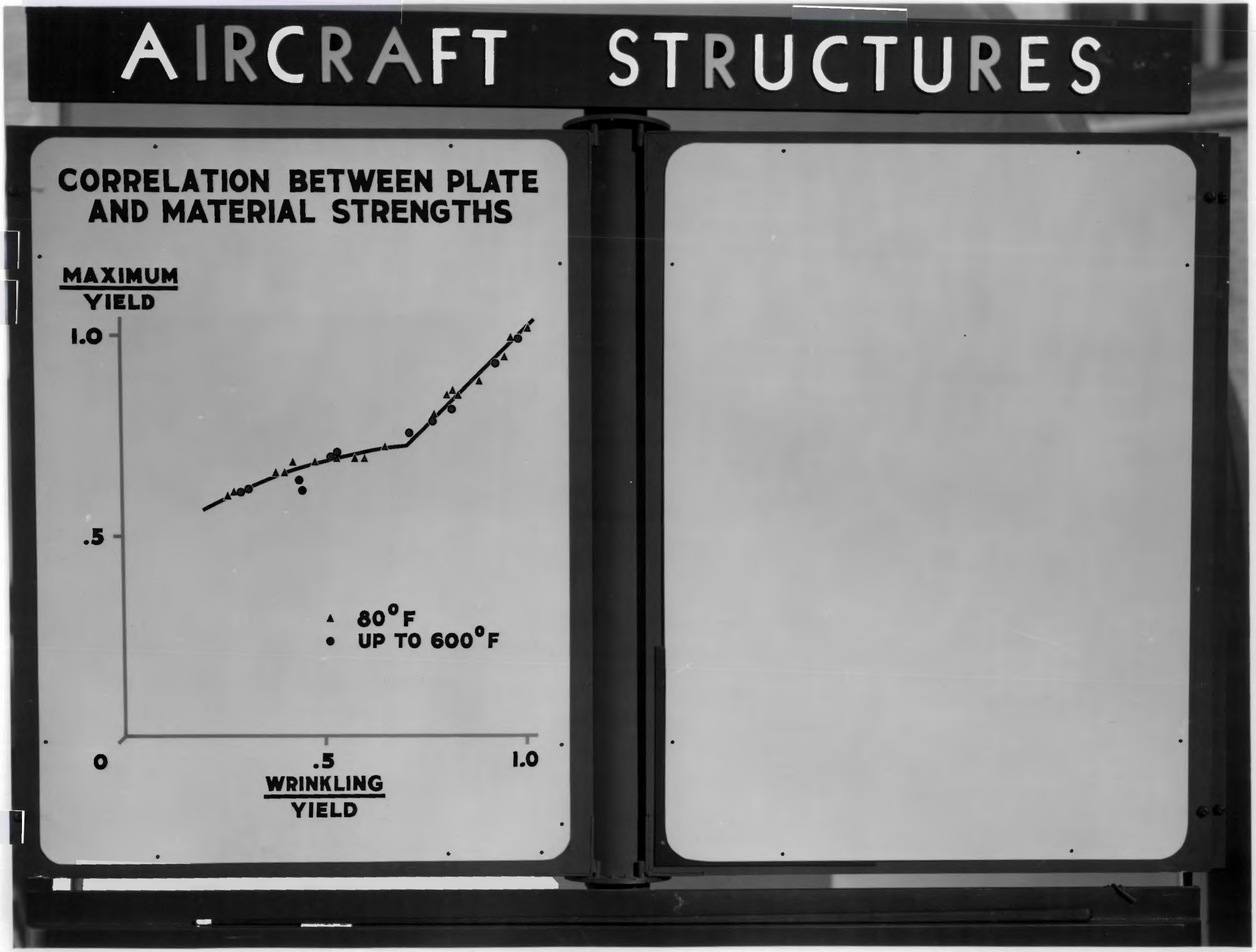

NACA
LAL 70600

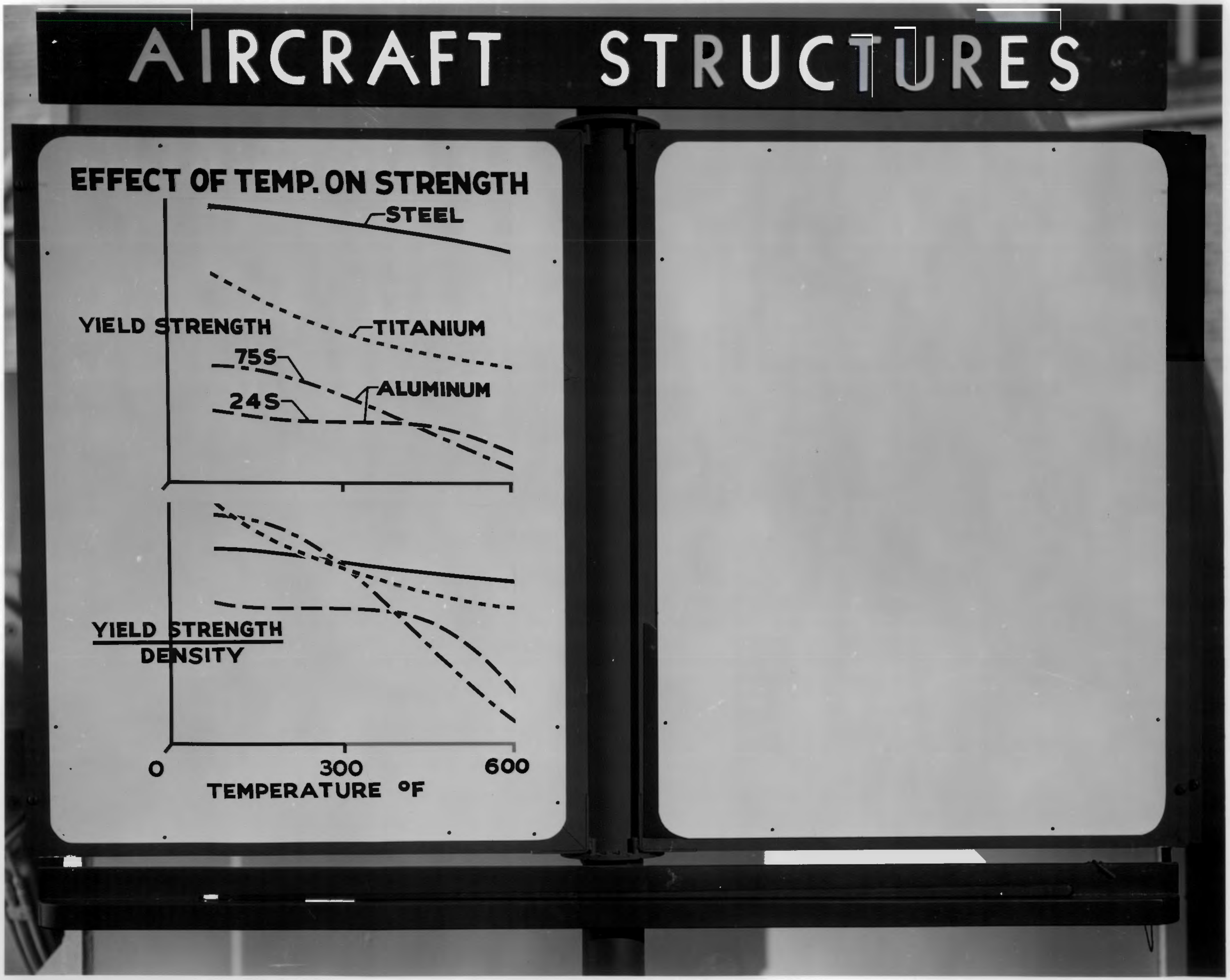

NACA
LAL-70601

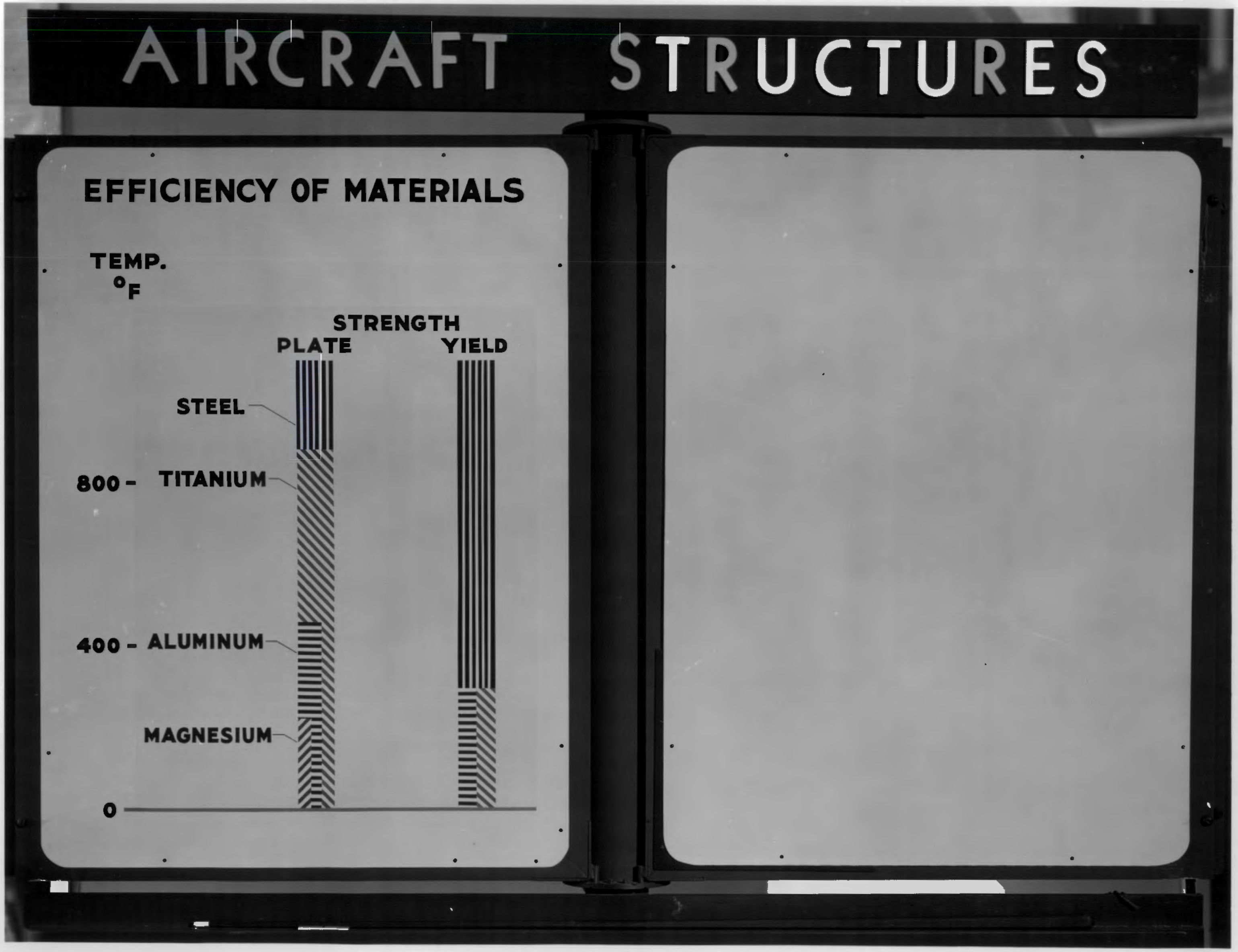

NACA
LAL 70603

1951 BIENNIAL INSPECTION

THE VIBRATION OF DELTA PLANFORM WINGS

Presented by

J. E. Anderson
Eldon E. Kordes
J. N. Kotanchik
Edwin T. Kruszewski
Manuel Stein

Many of you are no doubt aware that the wing configurations of very high speed aircraft are tending to become quite different from those to which we have become accustomed. The requirements of high speed flight are dictating the use of planforms such as delta wings, arrowhead wings, and very low aspect ratio swept wings. Although the wing shapes may be new, the old dynamic and aeroelastic problems such as flutter, landing impact, and gust loads still remain with us, and indeed their importance for very high speed airplanes may be accentuated. It is necessary therefore that we be able to analyze accurately the dynamic behavior of wings of the delta type. The analysis of such wings presents us with a whole new problem because the structural deformations of delta or arrowhead wings are very much different from those of the more conventional straight wings.

An ordinary straight wing vibrates very much like a long, slender beam - that is, it bends up or down, or it twists, or it does combinations of bending and twisting. These simple concepts of bending and twisting vibrations of a beam are not applicable to wings of the delta type, such as the one you see here. Structurally a wing of this type behaves like a flat plate rather than a beam. In a wing of this type each element of the plate, such as the squares which we have marked on the wing surface, can be undergoing a bending and a twisting motion about the spanwise direction or about the chordwise direction, and at any given instant the bending and twisting action of one element may be appreciably different from that of its neighboring elements or of more distant elements in the plate. We will demonstrate this bending and twisting action very shortly.

From a theoretical point of view we are fortunate in that there does exist a fairly well established theory for bending of plates. Although the theory leads to extremely difficult calculations we have made progress in various approximate approaches that incorporate the plate theory but yet approach the level of simplicity of beam theory, with which most engineers are familiar.

In order to show you the deformations that a delta wing undergoes we will vibrate this wing in its first three natural modes of vibration. The first natural mode looks like a simple up and down bending motion; actually there does take place a twisting action but it is too small to be observed.

Now we will produce the second mode of vibration. The vibratory forces are applied by a mechanical oscillator which is attached to the top surface of the wing. In order to give you the effect of a slow motion picture of the deformations in this mode of vibration we will illuminate the lower surface of the wing with a stroboscopic light which flashes on and off at a frequency slightly different from the frequency of the wing vibration.

In this second mode of vibration at any instant that the inboard portion of the leading edge moves upward, the tip moves downward, thus there exists between the tip and the inboard portion a point of no vibration. The action of the trailing edge is similar to that of the leading edge with the point of no vibration located here. These two points of no vibration are at the ends of a line of no vibration, called the nodal line. The existence of this line will be demonstrated more clearly later.

Note that the square elements in the tip portion of the plate are experiencing a bending and twisting which is noticeably different from that of elements in other parts of the plate.

If you will now direct your attention to this one white chordwise line and compare it with reference to the straight edge you will observe that the plate deflects into a simple upward or downward curve. This type of deformation may be important from the aerodynamic point of view because it affects the flow of air over the wing.

We will now increase the frequency of the vibrating forces and develop the third mode of vibration. In this third mode of vibration note that at any instant the entire leading edge is moving upward or downward. The action of the trailing edge in this mode, however, is similar to that of the second mode with the point of no vibration located here. The nodal line extends from this point through the center of the plate and into the root.

Again notice the dissimilar bending and twisting actions of square elements in various parts of the plate.

The straightedge now indicates that the plate is bending in an S-shape rather than a simple curve.

In order to show more clearly the presence of the nodal line, sand will now be sprinkled on the top surface of the plate; observe in the mirror above the wing that the sand bounces off the vibrating portions and collects along the nodal line.

We will now lower the frequency of vibration to obtain again the second mode of vibration. Observe in the mirror that the sand will move to a new position on the wing surface and define the nodal line for this mode of vibration.

It is only by understanding the distortions such as those we have shown you in this demonstration that designers can proceed with greater confidence in the design of safe and efficient structures of the delta type.

Gentlemen, this concludes the program in the Structures Research Division. Please follow your group leader out this way.

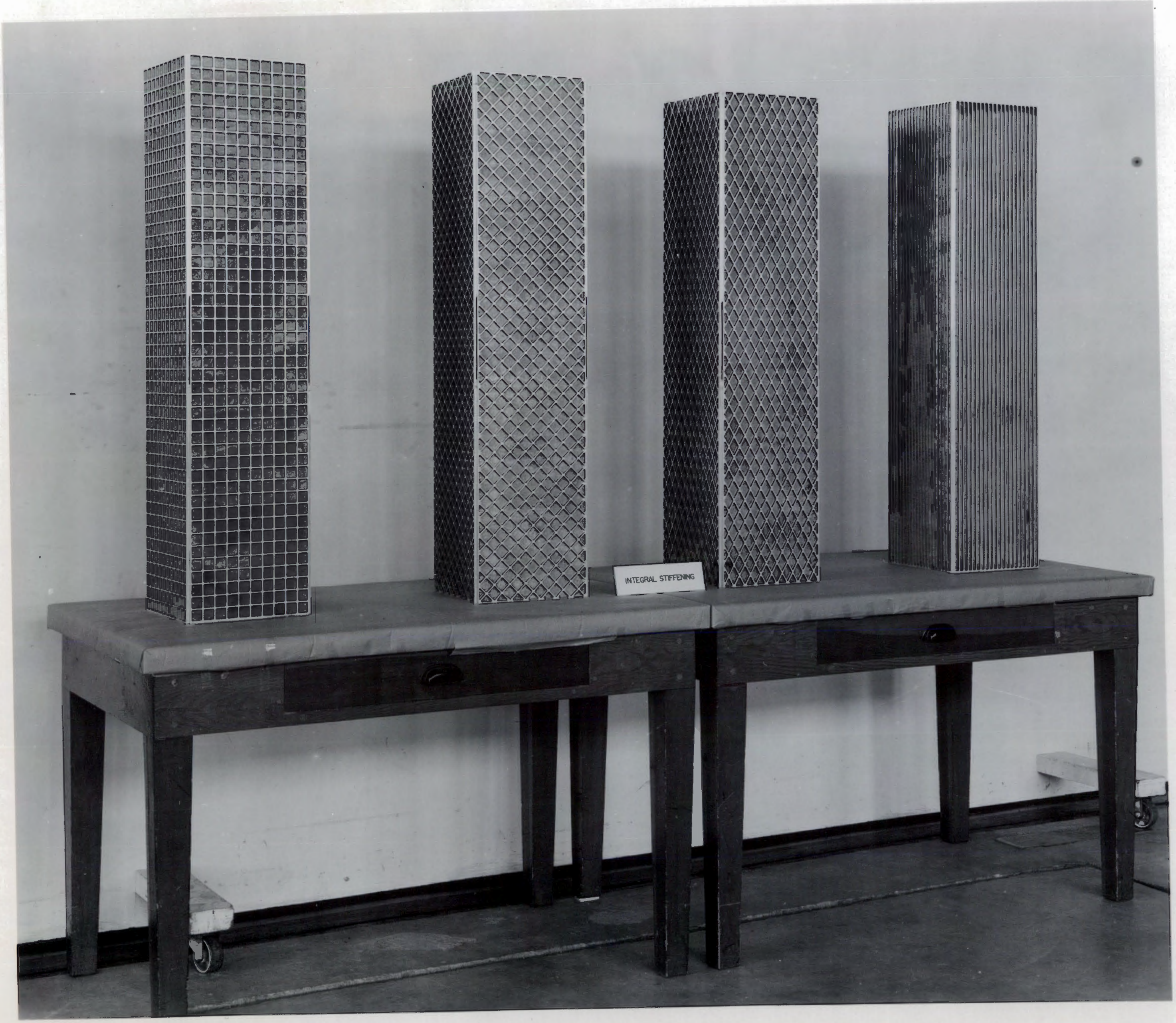

NACA

LAL 70593

NACA
LAL 70595

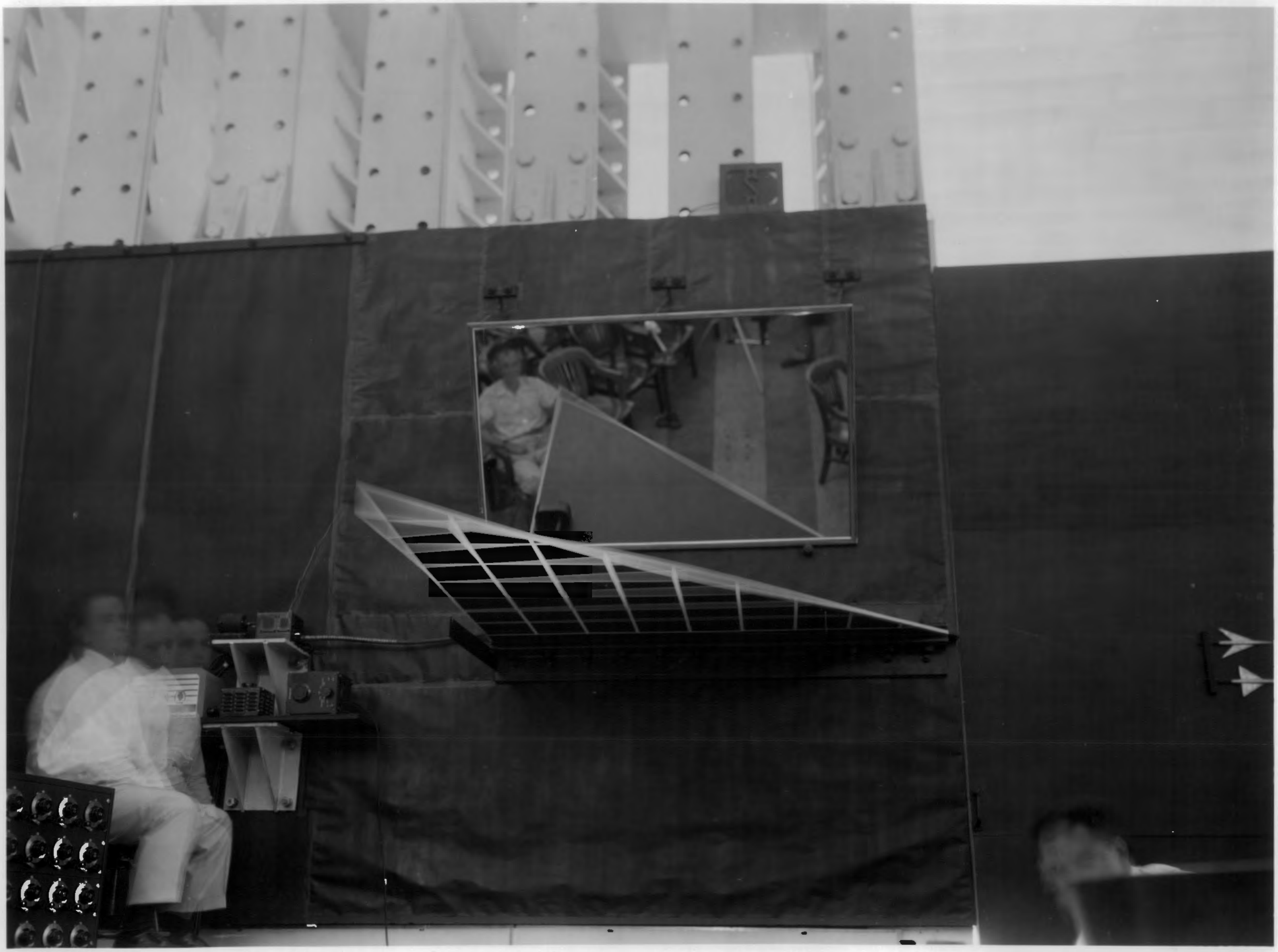

LAL 70596

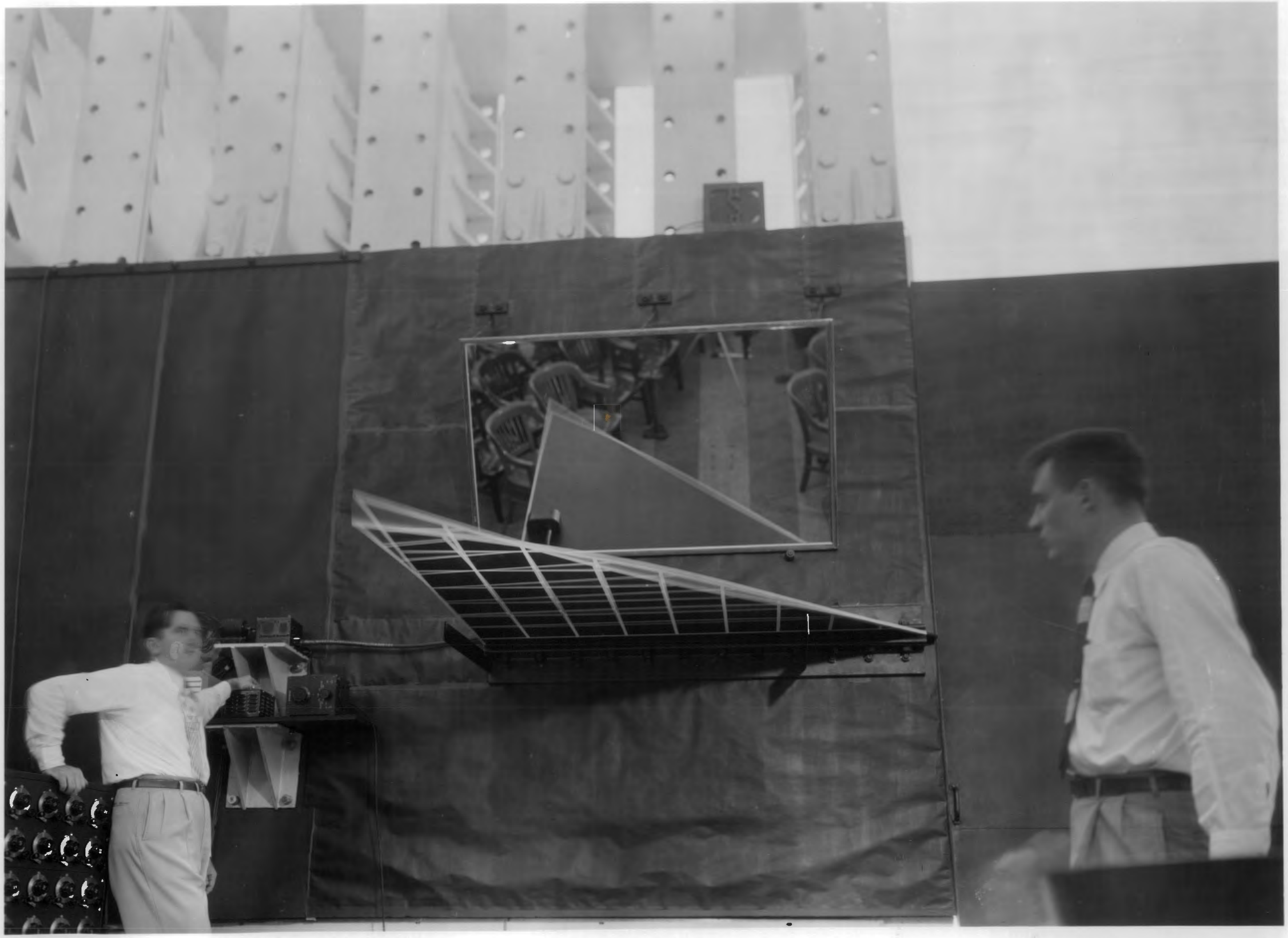

LAL 70597

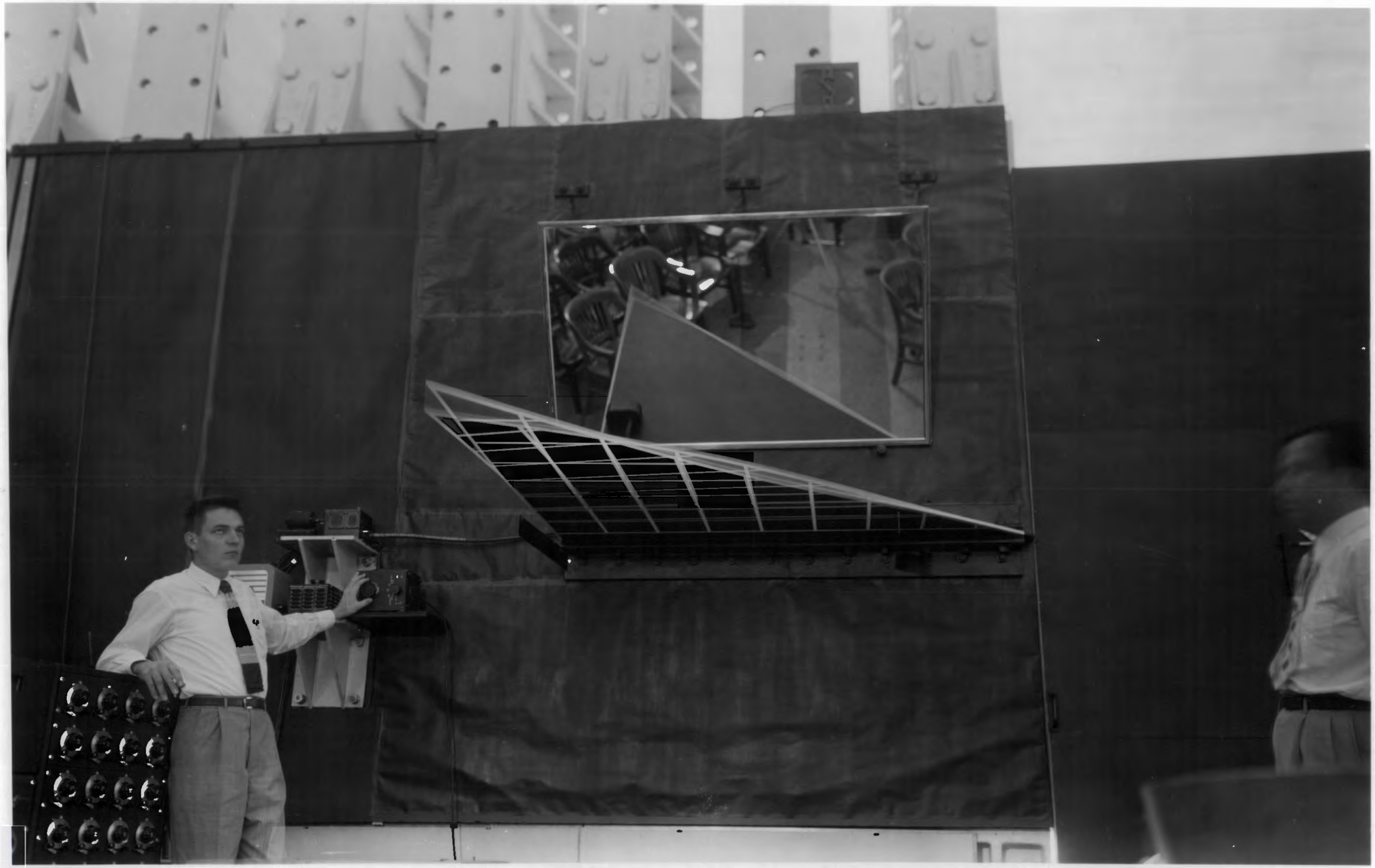

NACA
LAL 70598

LAL 70599

NACA
LAL 70560

WIRE STRAIN GAGE BALANCES
CHORD FORCE
YAWING MOMENT
ROLLING MOMENT

LAL 70572

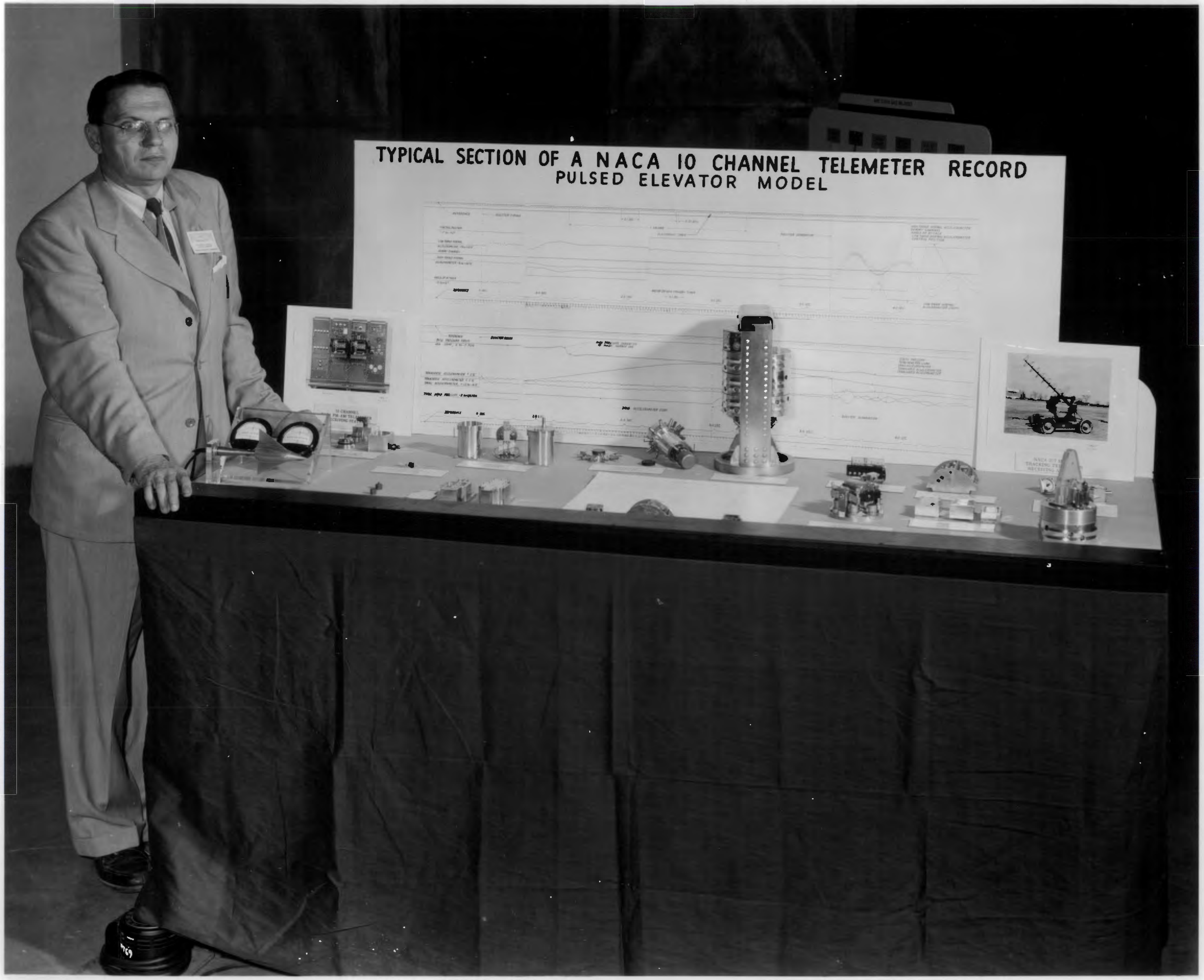

NACA

LAL 70573

NACA

LAL 70574

NACA

LAL 70570

NACA

LAL 70571